Materials Transactions, JIM, Vol. 36, No. 2 (1995), pp. 110 to 122

Process Modeling of Mechanical Alloying *(Overview)*

T. H. Courtney

Department of Metallurgical and Materials Engineering, Michigan Technological University, Houghton, Mi. 49931, U.S.A.

Recent efforts at modeling the mechanics and dynamics of mechanical alloying are summarized. The modeling is described from two perspectives. One considers the deformation response and the fracture and welding tendencies of powder particles entrapped between colliding grinding media in an individual collision. We call this local modeling. Fundamental and phenomenological approaches to local modeling have been undertaken, and these are described here as are numerical applications of the approaches. We have termed the second type of modeling "global modeling". Global modeling concerns itself with device specific characteristics, and has potential for improving MA devices. Global modeling also serves to provide parameters that are necessary to best utilize local modeling.

(Received November 2, 1994)

Keywords: *mechanical alloying, powder metallurgy, process modeling, particulate materials*

I. Introduction

In this paper I attempt to provide an overview of mechanical alloying (MA) modeling studies. Per request of the editors, this overview summarizes studies undertaken by several former students of mine. The modeling described deals with the mechanics and dynamics of MA, and the effect these have on alloying kinetics and the characteristics of processed powders. The approach I take here is parochial on at least two accounts. First, by focusing primarily on studies with which I have been involved, short shrift is given to others who have also been involved in similar work. And, as mentioned, most of the modeling with which I have been associated is concerned with "mechanical" effects. It does not deal with development of criteria for "predicting" the occurrence during MA of amorphization, material synthesis, chemical diffusion, etc. These lines of inquiry are paramount for full utilization of this intriguing process. It is appropriate at the outset to at least acknowledge some of these other contributions; a partial listing is given in Refs. (1)-(12).

II. Why Model Mechanical Alloying?

Modeling of MA is undertaken for the purposes of identifying the most salient factors affecting the process. If this is done successfully, empirical studies aimed at optimizing the efficiency of a specific application can be reduced substantially. In addition, process models are of use for establishing process control instrumentation. When viewed in these ways, process modeling of MA is similar to modeling of other processes.

It is necessary to appreciate what "information" can and cannot be expected forthcoming from such modeling. For one thing, "exact" answers will not be had; MA is too complex for that. Moreover, the frequency and velocity of "effective" impacts taking place during MA can only be approximately ascertained. And the thickness of the powder coating the media or entrapped between them during impacts (this thickness controls powder volume "treated" during a single collision and affects the deformation experienced by the powder and the tendencies for powder particle welding and fracture) is also only approximately known. Furthermore, material mechanical properties under the high strain and strain rate conditions common to MA are not known with precision. There is also an operational constraint. Models must be kept "simple" while still reflecting the fundamental physics of the process. For example, major efforts (*e.g.*, sophisticated finite element programs) are required to analyze fully and accurately the deformation response of powder particles affected in a specific collision. The same holds for analyses of the welding and fracture events the powder particles undergo. Given the uncertainty in the material property data base, such efforts are hardly worthwhile in terms of the incremental accuracy they provide.

We have attempted to develop "simple" models which provide physically plausible descriptions of the deformation response and welding and fracture proclivities of powder particles during MA. If the underlying physics of the model are correct, the models predict the general trends of powder particle development during MA. The models will also identify the effects of alterations in process variables on the trends in particle powder development. Empirical adjustments can then be made to improve processing and the operational usefulness of the models.

Thus process modeling of MA is similar in some respects to modeling of hot isostatic pressing (HIPing) and superplastic forming. In modeling of HIPing, geometrical approximations pertaining to the powder particle array are made; these facilitate analysis[13][14]. However, the basic physics of densification are maintained in the model. The model is then used to predict densification behavior as a function of the time, pressure and temperature employed. "Exact" results require accurate ancillary data; *e.g.*, surface energy, diffusion

coefficients and parameters in the constitutive laws for high temperature deformation. Many of these are not accurately known. The uncertainty in them can lead to a greater "error" than any arising from the geometrical approximations of the model. However, by delineation of parametric dependencies the model allows for extraction of the required data base by a selected few experiments.

Superplastic forming is routinely carried out with the aid of robust process models which are based on empirical and fundamental reasoning. Trial runs suffice to determine the constants in the models that are apropos to the specific material. The model can then be used for interpolation and extrapolation, as well as serving as a process control tool.

Thus almost all process modeling is not exact, but approximate. A "good" model identifies variables that importantly affect the process outcome. What we can reasonably expect from such a model is a reduction in empirical studies and a better chance at process optimization. In the long run, a "good" model is also necessary for *in situ* process control.

III. Modeling Philosophy

We have (somewhat arbitrarily) divided modeling of MA into two categories. In one, termed local modeling, we consider a "typical" collision involving powder trapped between grinding media. We specify a machine specific frequency and velocity of these collisions. Other process variables, such as CR (=media mass/powder mass: CR affects the powder coating thickness, h_0; increases in CR decrease h_0 and vice-versa) and certain mechanical characteristics of the powders are additionally stipulated. For a specific collision, we determine: (1) the deformation the particles experience; (2) the change in powder particle shape; (3) the probability of a particle coalescing; and (4) the probability of a particle fracturing. The "analysis" therefore provides a "snap shot" of the collision. A computational program has been developed that tracks the "average" powder particle over a series of "typical" collisions. This permits determination of a number of particle characteristics (shape, size, hardness, microstructural scale) as a function of the number of impacts the particle experiences. If the collision frequency is known, these characteristics can be "predicted" as a function of milling time.

The most important process parameters needed to render such modeling fruitful are the collision velocities, frequencies and powder coating thickness. These are estimated by "global modeling." This modeling considers heterogeneous aspects of MA. For example, powder is nonuniformly distributed in an attritor (most of the powder is situated in a region where milling action is minimal). The appropriate "average" velocity and frequency for an attritor are estimated by considering both the heterogeneous distribution of powder and the distribution in collision velocities. There is also a wide distribution in the impact energy dissipated during media collisions in a SPEX mill. Care must be taken here in extracting the frequency and velocity of "effective" collisions for use in local modeling. We mention that the velocities and frequencies we extract from global modeling, and which we have used in local modeling, are only "educated guesses."

We have also undertaken a different approach to local modeling, as exemplified in the studies of Aikin. These describe alloying "kinetics" from the standpoint of chemical kinetic principles. Alloying of two ductile materials to form a third (composite or alloy) species is considered. Welding and fracture probabilities of the constituent and alloy species are defined, and time evolution equations for the species developed using these parameters. The equations can be solved numerically and the appropriate welding/fracture constants extracted from parallel experimental studies. The approach appears different from that of Maurice's, described immediately above. However, the main difference between the approaches is that the fracture and welding probabilities are time dependent in Maurice's treatment, whereas they are considered constant in Aikin's.

This paper develops along several lines. Local modeling is first described. Maurice has recently developed an extensive description of MA, one that includes specifications for powder particle deformation, welding, and fracture. However, his initial treatment of MA is simpler. It only considers the powder deformation taking place during MA. Details of the mechanics of this deformation are also not treated in the depth they are in his more expanded treatment. Nonetheless, because the initial model contains within it much of the basic physics of MA and has the additional virtue of greater clarity resulting from simplified mathematics, we start with a review of Maurice's initial treatment. This is followed by a description of his more complete effort. Aikin's treatment is then described. We then review global modeling studies.

IV. Local Modeling

1. Initial treatment

Maurice[15] treated a collision between grinding media involving entrapped powder as akin to a Hertzian collision between balls absent the powder. It is reasoned that the powder only mildly perturbs such a collision; i.e., the plastic deformation (and other) work performed on the powder is assumed only a small fraction of the precollision media kinetic energy. If the assumption is correct the collision geometry and duration involving powder are comparable to those of a collision absent it. The assumption can be tested for consistency, as described below.

The geometry of a Hertzian collision between colliding balls is characterized by a maximum contact radius (r_h, the Hertz radius). This radius is attained at a time τ following collision initiation (the collision duration is 2τ). The Hertz radius and collision duration are given by

$$r_h = g_r v^{0.4} \left(\frac{\rho}{E}\right)^{0.2} R \tag{1a}$$

$$2\tau = g_\tau v^{-0.2}\left(\frac{\rho}{E}\right)^{0.4} R \tag{1b}$$

where $g_{r,\tau}$ are constants of order unity, v is the media collision velocity and R, ρ and E are the media radius, density and tensile modulus, respectively. Estimates on r_h range from tens to hundreds of μms, depending on v which is itself estimated to range between 0.5 m/s (*e.g.*, for an attritor) to 5 m/s (*e.g.*, for a SPEX mill). As indicated in eq. (1b) collision durations are not as sensitive to velocity as are contact radii. Collision durations are believed to be on the order of 10^{-5} s.

Powder trapped between colliding media deforms plastically. The powder volume affected is treated as a cylinder of radius r_h and height h_0. The velocity at which the powder deforms is assumed to decrease linearly from v (at collision initiation) to zero (after an elapsed time τ). The instantaneous powder strain rate is the velocity divided by h_0. Thus the process can be considered as "microupsetting." Strain rates are comparable to those in conventional upsetting. Taking h_0 as 100 μm[†1], maximum strain rates (which occur at impact initiation) are on the order of 10^3 (for $v=0.5$ m/s) to 10^4 (when $v=5$ m/s). Integration of the strain rate from $t=0$ to $t=\tau$ allows the deformation strain in a single collision to be calculated as[†2]

$$\varepsilon = -\ln\left(1-\frac{v\tau}{2h_0}\right). \tag{2}$$

Estimated powder strains range from several tenths of a percent (for an attritor) to unity (for a SPEX mill with a high CR). As mentioned, the model can be checked for self-consistency by comparing the magnitude of the precollision kinetic energy to the powder plastic deformation work. The latter is the powder affected volume multiplied by the integral of the powder's true stress-true strain curve over the collision duration. Using reasonable values for the flow stresses and work-hardening behavior of common metals, it can be shown that the powder deformation work is much less than the precollision kinetic energy.

In a later treatment, Courtney and Maurice[16] estimated processing times by assuming that a critical amount of powder deformation (Σ) is needed to accomplish alloying[†3]. The number of impacts therefore needed to "alloy" scales with Σ/ε. The time between collisions varies as v^{-1}. That only a small fraction of the powder "associated" with a given media ball is involved in each collision must also be taken into account when estimating processing times. The greater the powder affected volume ($=\pi r_n^2 h_0$) the less the required alloying time, other factors being equal[†4]. For $v\tau/2h_0 \ll 1$, $\varepsilon = v\tau/2h_0$. The alloying time, t_p, should vary as

$$t_p \sim \frac{\Sigma h_0}{v\tau r_n^2 h_0}. \tag{3}$$

Using eq. (1) for the velocity dependencies of the collision time and radius it can be shown that the alloying time depends on precollision velocity as

$$t_p \sim v^{-2.6}. \tag{4}$$

Equation (4) should be kept in mind when results of more ambitious descriptions of MA are provided later.

Although this initial MA model has been superseded by a later treatment, the essential features of the deformation process are well described by the initial model. That is, the subsequent treatment finds that the powder deformation per collision, the radius of the powder affected volume and the effective impact duration do not differ all that much from their values predicted by the initial treatment. This expanded treatment is now summarized.

2. A more ambitious treatment

Maurice's initial model did not consider criteria for, nor the frequency of, powder particle fracture and welding. In addition, the initial treatment provides a "snapshot" of a single collision; no attempt at a temporal description of MA is made. Maurice considered these additional factors in his Ph. D. thesis[17] and in several publications resulting from it[18][19]. The initial portions of this section encapsulate his thesis; interested readers may wish to consult it for details. The later parts of this section provide examples of how modeling can be used for process analysis and optimization.

(1) A single collision

For convenience Maurice considered a grinding media ball to be uniformly coated with powder[†5]. Powder particles subject to MA are generally not spherical in shape. Maurice took them to be oblate spheroids having minor (b) and major (c) axes; the particle shape factor is defined as $f_s = b/c$. During a collision the particles are presumed arranged on the ball surface as indicated in Fig. 1; i.e., the major axes of the particles are parallel to this surface.

The stages of impact when coated balls collide are indicated in Fig. 2. The balls initially deform elastically, and the stress they experience is greatest at the initial contact point (Fig. 2(a)). As the powder proceeds to deform, the stress here eventually attains the powder's yield strength and powder plastic deformation commences. With continuing deformation the radius of the plastic zone spreads radially outward (Fig. 2(b)). Thus the powder-affected-volume consists of a plastic cylindrical core sur-

[†1] The assumption is not arbitrary. Simple experiments[15] suggest this value of h_0 is reasonable.

[†2] The analysis is valid only when $v\tau/2 \ll h_0$. If this condition does not hold, the assumption concerning the relative magnitudes of the powder deformation and precollision kinetic energies is incorrect.

[†3] This assumption is also reasonable. Alloying of two-phase materials is accomplished by particle cold-welding (itself relying on particle plastic deformation). Particle fracture tendencies primarily determine processed particle sizes. Thus to a reasonable first approximation, MA of ductile materials is "finished" when the powders have been deformed a critical amount.

[†4] They are not. The strain per collision decreases with increases in powder affected volume[15].

[†5] In the numerical applications Maurice took h_0 as 100 μm. However, h_0 is a variable that can be altered in these programs.

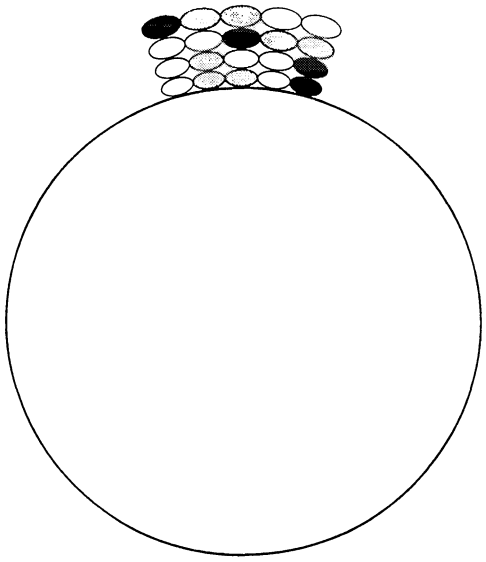

Fig. 1 Maurice's MA treatment assumes individual powder particles to be oriented on the grinding media surface such that the particle major axes are parallel to the surface (sketch not to scale). The differently shaded particles represent different powder species. From (18).

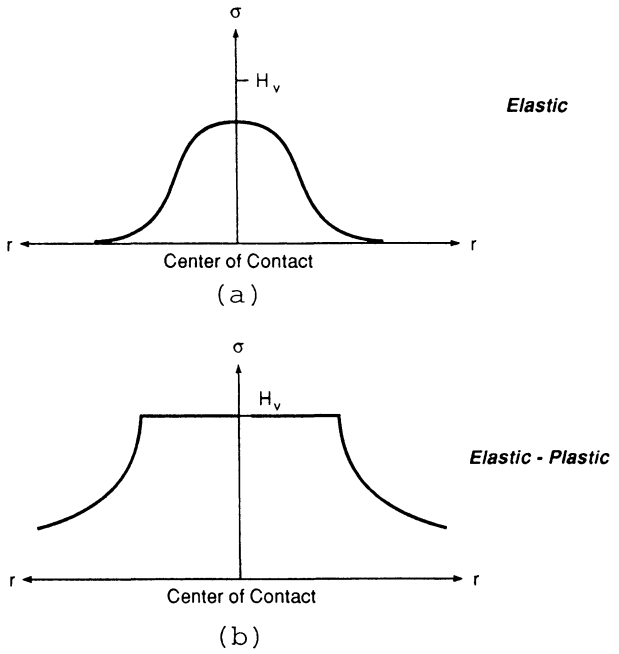

Fig. 2 The collision stages of powder coated balls. (a) In the early collision stage, the powder deforms elastically; the stress is greatest at the initial contact point. (b) When the stress at the initial contact point attains the powder hardness, plastic deformation initiates there and proceeds radially outward. Thus the contact zone is characterized by a plastic cylinder surrounded by an elastic annulus. From (18).

rounded by an elastic annulus. The strain the powder undergoes depends on the value of the center-to-center approach of the balls ($\alpha(r)$) which is a function of the distance (r) from the contact center. Maurice shows that $\alpha(r)$ is given by

$$\alpha(r)=Rv\left(\frac{\rho}{H_v}\right)^{1/2}-\frac{r^2}{R} \tag{5}$$

where R is the ball radius, v the precollision velocity, H_v the powder hardness and ρ the grinding media density. The center-to-center approach increases with v, decreases with H_v and, of course, is at a maximum at $r=0$[†6].

The center-to-center approach determines the true strain experienced by the powder, and this strain is expressed as

$$\varepsilon(r)=-\ln\left\{1-\frac{\alpha(r)}{h_0}\right\}. \tag{6}$$

The maximum strain (at $r=0$) is

$$\varepsilon(0)=-\ln\left\{1-\frac{Rv}{h_0}\left(\frac{\rho}{H_v}\right)^{1/2}\right\}. \tag{7}$$

If h_0 is independent of R, the strain increases with R. In the more likely event that h_0 increases linearly with R, the strain is independent of the grinding media size. Comparison of maximum strains calculated with eq. (7) to those resulting from the initial MA model are given in Table 1, which also provides other comparisons between the approaches. The correspondence between parameters of the approaches is fairly good, indicating that the physics underlying the initial model are realistic.

Due to work-hardening, powder hardness increases during MA. Therefore the incremental powder strain in successive collisions becomes progressively less. In numerical implementation of the model, the powder hardness is considered constant during a specific collision, but a hardness appropriate to a succeeding collision is estimated using the strain from the previous collision and an appropriate hardening law. Thus numerical analysis permits powder hardness to be "tracked" during processing.

Maurice assumes powder coalescence to take place by cold-welding of plastically deformed particles (Fig. 3). His analysis is based on previous treatments of cold-welding[(20)-(22)], and the physics are summarized as follows. The

Table 1 Comparison of parameters obtained with simplified MA model to those of more detailed treatment.

Parameter	Detailed treatment	Simplified model
Center-to-center Approach of balls (μm)	26	12
Contact radius (μm)	177	199
Powder strain	0.3	0.27
Impact duration (10^{-5} s)	2.44	1.5

Notes: Original model for Cu, with Cr=10 and coating thickness of ca. 50 μm. Detailed treatment for coating thickness of 100 μm. Particle hardness of 1 GPa. Values of approach and strain for detailed treatment appropriate to contact center; Values of approach and strain for original model are average values.

[†6] The analysis is valid only when some minimum quantity of powder coats the balls; that is, $\alpha(0)<h_0$. The restriction is similar to that noted in footnote †2. The analysis is also not valid when the powder hardness is equal to or greater than the grinding media hardness.

particles are presumed initially coated with a brittle oxide film. The brittle film is fractured during deformation, and metal-metal contact established between particles. The surface area of the exposed metal increases with particle plastic deformation, and the degree of metal-metal mating across contacting surfaces is determined on a statistical basis[17].

A weld, once formed, may not survive the elastic recovery associated with the last half of the collision, and which produces a tensile stress acting to sever the weld. A shear stress, present in other than "head-on" collisions, also serves to shear the weld (Fig. 3). Maurice used an effective stress argument to define the criterion for weld "survival";

$$\sigma_u^2 A_w^2 \geq N_e^2 + 3T_b^2 \tag{8}$$

In eq. (8) A_w is the area over which metal-metal contact has been made, σ_u the weld tensile strength, N_e the normal elastic recovery force and T_b the comparable shear force. Maurice also considered the presence of dispersoids entrapped between the mating surfaces. The dispersoids impede welding by reducing the area over which metal-metal contact is made. Knowing the dispersoid size and number density permits calculation of the appropriate area reduction and stipulation of a redefined welding criterion.

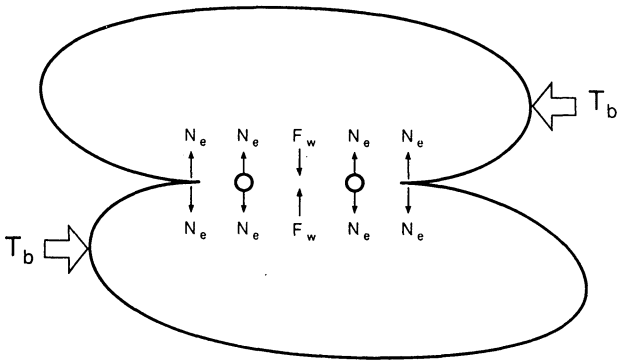

Fig. 3 Schematic of powder cold-welding during MA. Plastically deformed particles make metal-metal contact over a fraction of their mating area. The weld formed may or may not survive the recovery half of the collision; this depends upon the strength of the formed weld relative to the elastic recovery force (N_e) and the shear force (T_b) (present when the collision is other than a head-on collision) serving to sever the weld. Dispersoids (open circles) act to prevent cold-welding. From (17).

[17] For alloying different materials, this treatment requires that both materials deform before a weld forms between them. Thus, if the starting hardnesses of the materials differ substantially, coalescence between them does not occur until the initially softer material is work-hardened to a hardness equal to that of the initially harder species. "Encapsulation" of the hard species by the soft one is an alternative mode of cold-welding, and encapsulation is frequently observed in powders milled in low power devices, such as an attritor, *e.g.*, (23). Some ramifications of not considering the encapsulation mode of coalescence are discussed later.

Criteria for fracture initiation and propagation were also developed. The essential ideas follow. After considering several different possible fracture initiation modes, Maurice concluded that "forging" fracture-as common to ordinary upsetting-was most likely to initiate fracture. Two methods were developed for determining a fracture initiation criterion. The first, based on macroscopic models of forging and which invoke sticking friction and workpiece barreling[24], predicts strain is greatest at the particle circumference. Thus edge fracture initiates there. The second method disregards sticking friction. Strain is greatest at the contact center and crack initiation is predicted to take place at the particle center, as might be expected for a brittle material. Although the first method is more physically plausible for fracture of ductile materials, little differences in the crack initiation strains were found for the two methods. Since the second method resulted in a more tractable solution, it was used in the computational models subsequently developed. Furthermore, when uncertainties in material mechanical properties are taken into account, the relatively small differences in predicted critical fracture initiation strains can be considered insignificant.

The initial crack length is taken as the distance over which the threshold fracture strain is exceeded. If this length is less than the powder particle size, the crack must subsequently propagate to effect particle fracture. Maurice used the J integral approach to define a propagation criterion.

Maurice also considered powder particle shape changes due to particle deformation, cold-welding and fracture. The particle shape factor is doubled by cold-welding and fracture, but is reduced by deformation. By following the particle deformation, fracture and cold-welding over a series of impacts, particle shape factor is tracked during processing.

The descriptions of cold-welding and, particularly, fracture are simplified descriptions. However, the physics of the processes are undoubtedly incorporated into the model. Cold-welding of ductile metal particulates requires their prior deformation, and the strength of the weld between them is surely related to the tensile strength of the joined materials. Moreover, fracture initiation takes place after a critical amount of prior deformation, and a fracture mechanical criterion for propagation of cracks thus formed certainly applies. Thus, irrespective of the "details" of the cold-welding and fracture events, the model is physically plausible and, because of its relative simplicity, is computationally robust.

(2) Computational development and applications

The model has been incorporated into computational programs. These provide a temporal description of powder size, microstructural scale and hardness during MA. The model can therefore be used for predictive purposes as well as for clarifying the role of important process variables on alloying behavior. Maurice developed two such programs. MAP1 is the simpler; it considers milling of a single species with the option of adding dis-

persoids. MAP2 is more sophisticated. It can be used for modeling the kinetics of MA of two species (A and B) to form a third (i.e., alloy) species (C).

MAP2 operates as follows. The number of particles trapped between colliding media is the powder collision volume ($=\pi f_p h_0 a_f^2$; a_f is the plastic contact zone radius and f_p is a volumetric packing factor (0.6–0.7)) divided by the average particle volume. The collision volume is divided into concentric annuli (100 in Maurice's treatment); the deformation, fracture and welding tendencies depend on radial position within this volume. In the numerical treatment it is assumed that only one welding and/or one fracture event per particle can take place in a given collision. The number of A-A, A-B, A-C etc. contacts is determined statistically to test for the frequency of the various kinds of weld. If an A particle welds to another particle (regardless of species), the number of A particles is reduced by one; the same applies to B and C species. When an A particle welds to a B particle, the number of C particles is increased by one. And when any particle species fractures the number of that species is increased by one. The particles are "counted" following each collision, and the numbers are used for the analysis of the subsequent collision.

MAP2 also determines deformation as a function of radial position in the contact zone. A model premise is that the harder of the species does not deform (and therefore weld or fracture) until the softer species is work-hardened to a hardness equal to that of the initially harder species. After this has occurred, the program incrementally deforms one of the species (the softer one to begin with), calculates a new hardness and deforms the harder species to match. Particle shape factors, altered during the collision by deformation, welding and fracture, are determined. If the new shape factor exceeds one, its inverse is used as the value of f_s in the following collision (cf. Fig. 1). Following each collision, the program also determines particle size, hardness and number for the various species and, for the alloy particle, the interlamellar spacing. Some examples of program application are provided in the following.

Benjamin and Volin[25] investigated MA of SPEX milled elemental Fe-Cr powders. The stages of alloying they observed are prototypical of those in many malleable metal systems. Thus their study provides a reasonable "test" of the model. Figure 4 shows the milling time variation of the welding and fracture frequencies predicted by numerical analysis using Maurice's model[†8]. As shown in this figure, predicted welding frequencies exceed predicted fracture frequencies for about the first 12 min of processing. Thus particle size should increase for the first 12 min of alloying and decrease thereafter. Comparison with experiment is provided in Fig. 5. The maximum in average particle size (ca. 100 μm) is somewhat less than that predicted by the model (ca. 130 μm), and the time at which the maximum is observed (30–40 min) is about three times longer than the corresponding model predicted time.

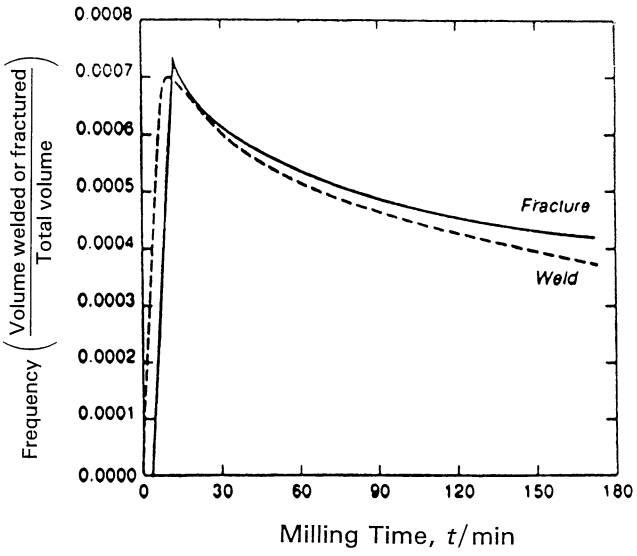

Fig. 4 Model computed particle weld and fracture frequencies for the Fe-Cr system studied by (25). Frequency units are volume welded/fractured per impact divided by the volume of powder associated with each grinding ball. Predicted weld frequencies exceed predicted fracture frequencies for the first 12 min of processing. Thereafter, the opposite holds. From (17).

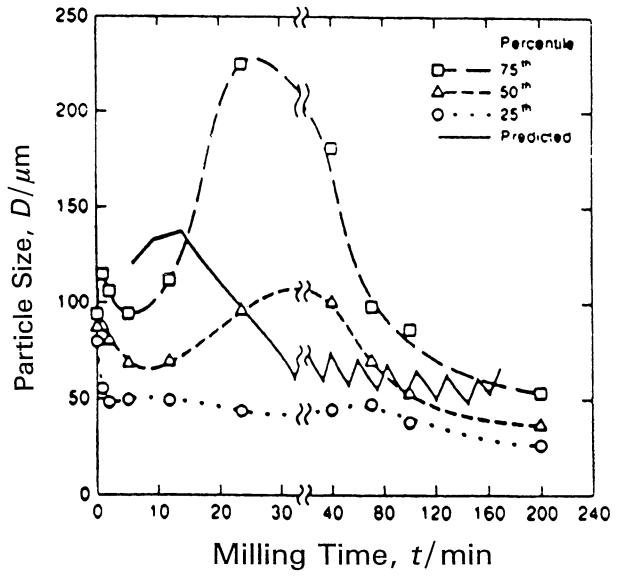

Fig. 5 Comparison of model predicted (solid line) and measured (25) particles sizes for SPEX milled Fe-Cr alloys (predictions should be compared to the measured 50th percentile). The model predicts a maximum in particle size somewhat larger than is experimentally found. The time at which the maximum size is predicted to occur (12 min) is less than the 30–40 min at which the maxium is experimentally observed. Measured and predicted "steady state" sizes are approximately the same. From (17).

Model predicted hardnesses are less than observed ones (Fig. 6). One reason for the discrepancy is the difficulty in formulating adequate constitutive laws for

[†8] Mechanical property data used are given in (19). This reference also discusses the sensitivity of model predictions to input property data.

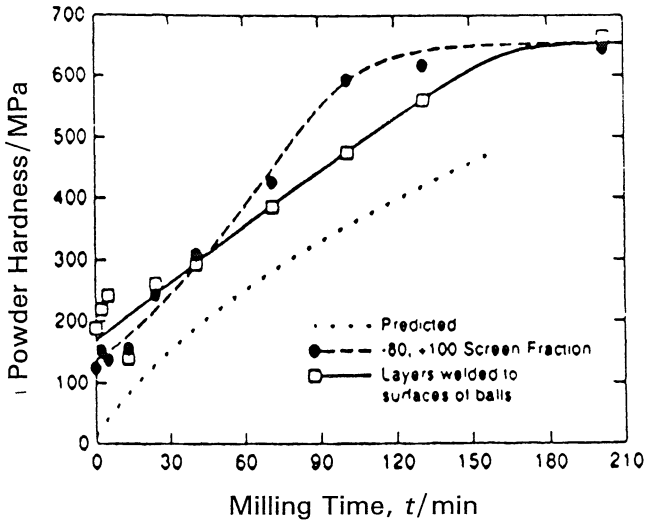

Fig. 6 Measured (25) and predicted (17) hardnesses for SPEX milled Fe-Cr. The trend in observed and predicted hardnesses is the same. However, predicted hardnesses are less than experimental ones. From (17).

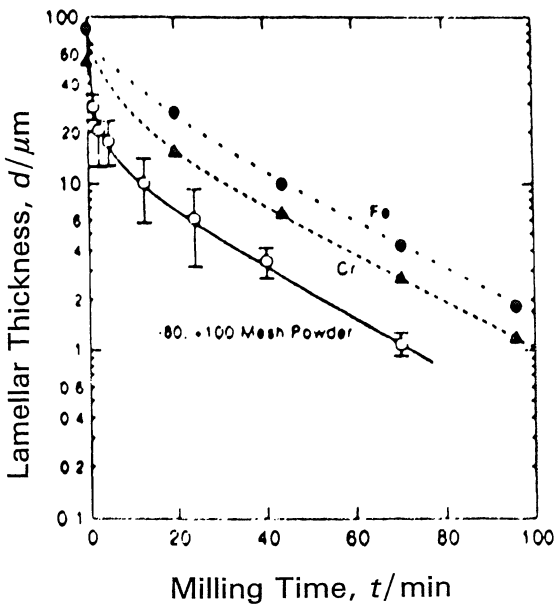

Fig. 7 Measured (open circles, (25)) and model predicted (dashed lines and filled symbols, (17)) lamellar thicknesses for mechanically alloyed Fe-Cr particles. The model predicts a coarser microstructure than is observed. Along with the hardness correlation of Fig. 6, this indicates the model underestimates powder deformation per impact. From (17).

heavily deformed two-phase materials; they are prone to manifest substantial additional high strain work-hardening relative to their single phase counterparts. If this factor is not taken into account, it appears the deformation per collision is underestimated by the model. This is also suggested on comparing measured and predicted interlamellar spacings (Fig. 7).

Although there are discrepancies between observations and "predictions"[†9], it is gratifying that predictions and experimental results are typically within a factor of two or three of each other. In addition, experimental results and predictions display the same trends. This suggests the model can be used (with empirical adjustments) for extrapolation (for example, to alloying with a different CR or with a more energetic mill).

Gilman and Nix[26] mechanically alloyed Al in a SPEX mill. Comparisons of their observations with model predictions are provided in Fig. 8. Predicted powder hardnesses exceed measured ones (at least at longer milling times), a discrepancy comparable to that for Fe-Cr alloys. Agreement between predicted and observed particle sizes is apparently quite good. Maximum particle size increases rapidly to about 100 μm; the model predicts a particle size maximum of 94 μm after milling for ca. 10 min. In addition, the measured particle size is 70 μm after 2 h of milling; the predicted size is 82 μm., There is an im-

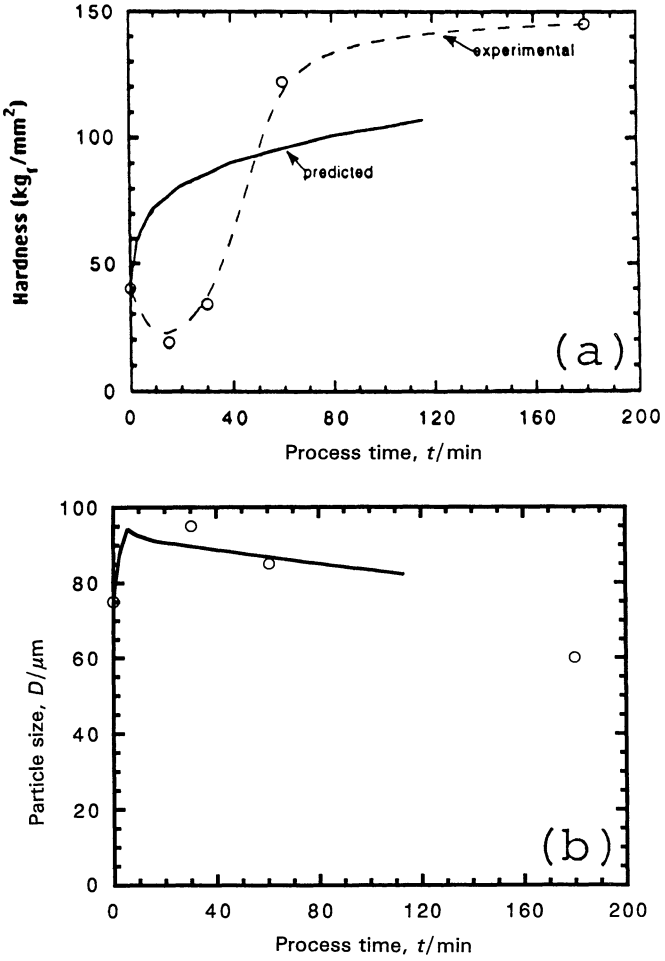

Fig. 8 (a) Model predicted and experimentally measured (26) microhardnesses of SPEX milled Al. For long milling times, predicted hardnesses are about 20% less than measured ones. (b) Measured (open circles) (26) and predicted (solid line) median particle sizes for SPEX milled Al. Measured and predicted sizes are in good agreement. A caveat is provided in the text. From (19).

[†9] We add that predictions were made with "first guess" estimates of material properties and process variables. That is, no "curve fitting" was done.

portant caveat here. Gilman and Nix used a process control agent (PCA) to prevent excessive mill caking: Model predictions did not consider PCAs; thus the model predicts a lesser welding frequency than that actually found in the absence of a PCA. The model can, of course, be "empirically" adjusted to reduce the welding frequency. In this case, the fractured alumina might be considered to behave as a dispersoid†10.

It is also possible to consider using the model to identify the role of process variables on alloying behavior, at least in a qualitative to semiquantitative way[19]. Consider alloying of two elemental powders (A and B) to form alloy (C) particles. We are interested in how collision velocity affects the alloying behavior of elemental constituents having different mechanical properties (see Table 2). The alloy identified as "0" in Table 2 consists of constituents with widely disparate starting hardnesses and moderately differing fracture toughnesses. The alloy sequence -1-2-3-4- designates that the properties of the starting constituents are made progressively similar.

Figure 9 shows the predicted (particle number) fraction of the powder population that is alloy particles after eight "effective" impacts. As expected, higher collision velocities result in more rapid alloying. There is a pronounced effect of material property differences on alloying kinetics; materials having similar starting properties alloy faster. A reason for this is that the model does not permit welding between different species to occur until their hardnesses are equal†11.

Processing times required to produce a powder population that is 95% alloy particles are shown as a function of collision velocity in Fig. 10. Differences in alloying times for the several material combinations are noticeable at low collision velocities, but hardly apparent at high velocities.

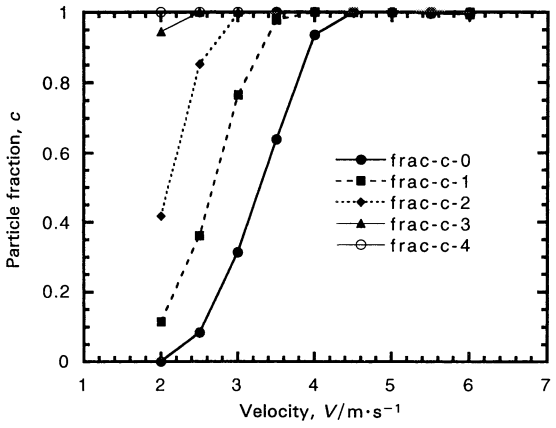

Fig. 9 Alloy particle number fraction of the powder population after eight effective impacts as a function of impact velocity for alloys 0–4 (properties listed in Table 2). Regardless of impact velocity, alloying is essentially complete for the elemental blend (4) having constitutents with comparable properties. In contrast, alloying has not begun at $v=2$ m/s for the blend (0) having disparate initial properties.

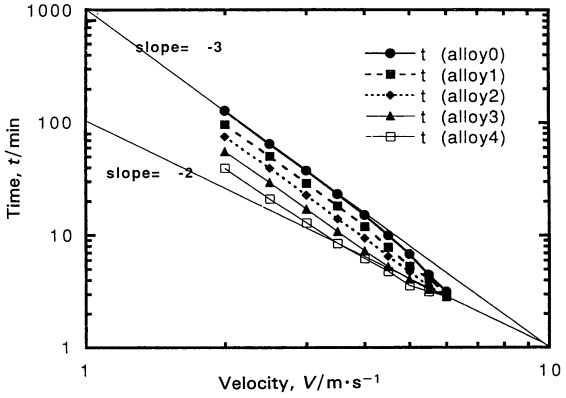

Fig. 10 Processing times required to produce a blend of 95% alloy particles as a function of impact velocity for the alloys of Table 2. Alloys with constituents having comparable properties require less processing time. Differences in required processing times are most notable at low impact velocities.

Table 2 Properties of starting materials used in study of alloying kinetics.

Alloy	0		1		2		3		4	
Property	A	B	A	B	A	B	A	B	A	B
Tensile strength (MPa)	275	580	306	550	336	519	367	489	397	458
Fracture strain	0.37	0.48	0.38	0.47	0.39	0.46	0.40	0.45	0.41	0.44
K_{Ic} (MN/m$^{3/2}$)	85	95	86	94	87	93	88	92	89	91
H_{vo} (KG$_f$/mm^2)	54	153	64	143	74	133	84	123	94	113
K (MPa)	275	140	262	154	248	167	235	181	221	194
n	0.42	0.50	0.43	0.49	0.43	0.48	0.45	0.47	0.45	0.46

Notes: Simulation done for CR=10. Material "A" had modulus of 170 GPa; Material B had modulus of 200 GPa. K and n are constitutive equation parameters.

Lines having slopes of -2 and -3 are drawn in Fig. 10. They reasonably bracket the "data"†12; a slope of -3 appears to fit best at low collision velocities and for materials with the greatest differences in starting hardnesses and a slope of -2 is better for blends of elements having comparable initial properties.

Particle size after eight impacts is shown as a function of velocity in Fig. 11. For the elements having the greatest difference in initial hardness, alloying has barely begun after eight impacts at $v=2$ m/s. This is reflected in a fine particle size (essentially the initial size). In contrast, alloying is essentially complete for $v=2$ m/s for the elemental combination having the most similar properties. This material combination manifests a large particle

†10 Recall that MAP1 allows for the presence of a dispersoid in the charge. Thus an advantage of MAP1 is that it can mimic the action of a PCA on welding frequency. (PCAs act similarly to dispersoids in terms of altering this frequency.)

†11 See previous discussion; the matter is also touched on later. However, even after making allowance for the possibility of "encapsulation" coalescence, it seems reasonable that longer milling times are needed to alloy materials with large differences in hardness.

†12 Recall earlier discussion of the "simple" MA model for which alloying time is predicted to vary with $v^{-2.6}$.

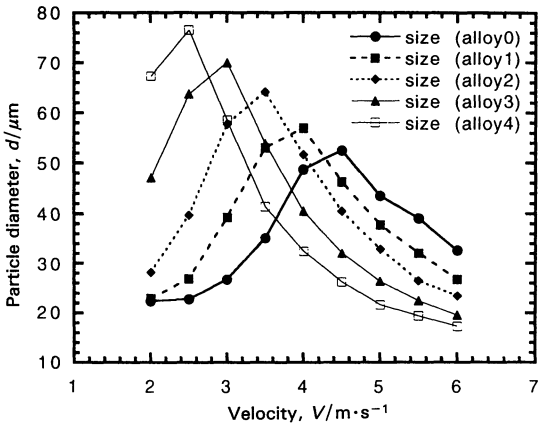

Fig. 11 Powder particle size after eight effective impacts as a function of impact velocity for the alloys of Table 2. Maximum processed particle size (which is found when alloying is essentially complete after eight impacts, cf. Fig. 9) is greatest for alloy 4; the blend having the most comparable initial constituent properties.

Table 3 Some input paramters required for numerical application of the model.

Material property	Precision known to
Modulus	High
Density	High
Initial particle size	High
Initial hardness	High
Tensile strength	Moderate
Fracture strain	Moderate to low
Fracture toughness	Moderate to low
Plastic flow law parameters	Moderate to low
Process variables	**Precision known to**
Charge ratio	High
Powder coating thickness	Moderate
Impact velocity	Moderate to low
Impact frequency	Moderate to low

Notes: For material properties-high precision means to several percent at best; moderate precision to 25% or so; low precision to a factor of two at best: For process variables-high precision means to several percent; moderate precision to a factor of two or so; low precision to about a factor of ten or less.

size, reflecting the cold-welding accompanying the formation of composite particles. Note that the maximum in particle size for each material combination is found approximately at the velocity needed to "alloy" in eight impacts. This maximum particle size is less for combinations having large differences in mechanical properties. This is caused by the additional powder deformation needed prior to welding (which causes fracture to occur earlier on) and/or the lesser fracture toughness of the more brittle alloy constituent.

The program has also been used to "predict" attritor alloying kinetics[17]. In distinction to the situation for SPEX milling, the model predicts alloying times much longer than those observed for attrition milling of materials with significantly different starting hardnesses[†13]. The cause is the model stipulation that welding does not begin until constituent hardnesses are equal. Coalescence by encapsulation is commonly observed in attrition milling of materials with significantly different hardnesses. Thus MAP2 should be expanded to handle situations like this.

In closing this section, it is worthwhile repeating the reasonable expectations of modeling of this sort and computational applications of it. The precision of the material properties and process parameters used in the computational applications varies, sometimes substantially. A partial listing of these properties and parameters is given in Table 3, which provides comments relative to the accuracy with which the properties/parameters are known or can be estimated. Some properties are known precisely (*e.g.*, modulus and density); others are likely known only to a factor of two at best (*e.g.*, hardening laws at high strain, fracture initiation strain, fracture toughness of milled powder). Processing variables (collision frequencies and velocities) are known even less accurately. Global modeling and "intuitive" extrapolations from such modeling provide "ballpark" figures for process parameters. Finally, coating thicknesses must be estimated; their approximated values are thought accurate to a factor of two or so. Global modeling can improve the accuracy of local modeling by providing refined values of the process parameters used in local modeling. Before proceeding to discuss global modeling, though, we describe the phenomenological approach taken by Aikin in her local modeling studies.

(3) Phenomenological modeling

Aikin's phenomenological description is based on kinetic principles[27]-[29]. The model has some critical assumptions, the most important being that the particle fracture and welding frequencies, while species dependent, do not depend on particle size or on milling time.

The basic idea is schematized in Fig. 12, which indicates how the populations of elemental starting powders (A and B) and alloy (C) particles change as a result of particle fracturing and welding. A welding probability is assigned to each possible coalescence event; *e.g.*, α_{AA} represents the probability per unit process time of two particles of A welding to each other, α_{AC} represents this probability for particles of A and C welding to each other, etc. Similarly, α_i represents the probability per unit time of a particle of species i (=A, B or C) fracturing. Using first order reaction kinetics the number of A particles (N_A) is shown to vary with milling time as

$$\frac{1}{N}\left(\frac{dN_A}{dt}\right)=\frac{f_A}{\tau_C}\{\alpha_A-f_A\alpha_{AA}-2f_B\alpha_{AB}-f_c\alpha_{AC}\} \quad (9)$$

where N is the total number of powder particles (of all species), τ_c the time between powder particle collisions and f_i the (particle number) fraction of species i. An equation similar in form to eq. (9) applies for B particles. The analogous equation for C particles is

[†13] The "error" in predicted alloying times scales with the number of impacts needed to appropriately harden the softer material.

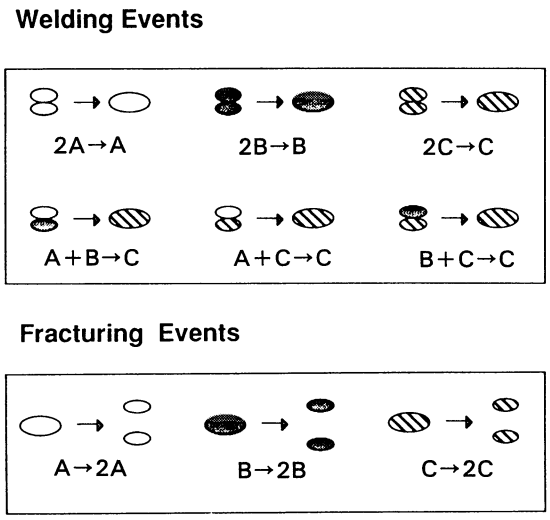

Fig. 12 Schema[28] showing how powder particle numbers change as a result of fracture and weld events. A and B particles are alloyed to form composite (C) particles. When an A/B particle welds to any other particle, the number of A/B particles is reduced by one. If an A particle welds to a B particle, the number of C particles is increased by one. When two C particles weld, the number of C particles is reduced by one. When any type of particle fractures, the number of that particle species is increased by one.

$$\frac{1}{N}\left(\frac{dN_C}{dt}\right)=\frac{1}{\tau_C}\{f_C\alpha_C-f_C^2\alpha_{CC}+2f_Af_B\alpha_{AB}\}. \quad (10)$$

Taking into account that both N_i and N vary with time, the time variation of f_A is expressed as

$$\left(\frac{\tau_C}{f_A}\right)\left(\frac{df_A}{dt}\right)=(1-f_A)\alpha_A-f_B\alpha_B-f_C\alpha_C-f_A(1-f_A)\alpha_{AA}+f_B^2\alpha_{BB}+f_C^2\alpha_{CC}-2(1-f_A)f_B\alpha_{AB}-2(1-f_A)f_C\alpha_{AC}+2f_Bf_C\alpha_{BC}. \quad (11)$$

A similar expression pertains for f_B, and the comparable expression for f_C is[†14]

$$\tau_C\left(\frac{df_C}{dt}\right)=-f_Af_C\alpha_A-f_Bf_C\alpha_B+f_C(1-f_C)\alpha_C+f_A^2f_C\alpha_{AA}+f_B^2f_C\alpha_{BB}-f_C^2(1-f_C)\alpha_{CC}+2f_Af_B(1+f_C)\alpha_{AB}+2f_C^2(f_A\alpha_{AC}+f_B\alpha_{BC}). \quad (12)$$

[†14] The number of parameters in the model can be reduced by use of approximations relating the fracture and welding probabilities of composite and elemental particles. For example, we could write $\alpha_C=V_A\alpha_A+V_B\alpha_B$; this approximates the alloy particle fracture probability as proportional to the volume fractions ($V_{A,B}$) of A and B in it. Probabilistic considerations also suggest:

$$\alpha_{AC}=V_A\alpha_{AA}+V_B\alpha_{AB}$$
$$\alpha_{BC}=V_B\alpha_{BB}+V_A\alpha_{AB}$$
$$\alpha_{CC}=V_A^2\alpha_{AA}+V_B^2\alpha_{BB}+2V_AV_B\alpha_{AB}=V_A\alpha_{AC}+V_B\alpha_{AB}$$

Aikin chose not to reduce the number of parametric variables by this procedure[23]; the "fit" to experimental data was not as good on doing so. Nonetheless I believe it is better to use a fewer number of variables, even if the resulting curve fit obtained from limited data is not as good. The tactic of minimizing the number of adjustable parameters is generally beneficial in kinetic modeling.

Note that for milling of an elemental species (*e.g.*, A) the number of powder particles varies with time as

$$\frac{N}{N_0}=\exp\left[\frac{(\alpha_{AA}-\alpha_A)t}{\tau_C}\right] \quad (13)$$

where N_0 is the initial number of such particles. Therefore measurement of the time variation of N allows the differences between the welding and fracture probabilities of the elemental species to be determined. This reduces (by two) the number of adjustable parameters in the model.

Aikin applied the model to attritor milling of elemental Cu and BCC transition metals (Fe, Nb and Cr) and to blends of Cu and the BCC metals[28]. Measurement of the time variation of the particle fractions of each species in the blends permits estimation of the several probabilities. This is done by curve fitting. An example of the resulting "fit" is shown in Fig. 13. Although the procedure is empirical, it has some advantages. For example, Alkin showed that the fracture and welding probabilities scale directly with CR and depend almost linearly on mill power.

Another use for it is its potential for predicting particle size distributions. On the model assumptions that the fracturing and welding probabilities are size independent, the temporal variation of particle size distribution during milling of an elemental species powders is represented by

$$\tau_C\left[\frac{dn(v)}{dt}\right]=-\alpha_An(v)-\alpha_{AA}n(v)\int_0^\infty f(v')\,dv'+2\alpha_A\int_v^\infty\frac{n(v')}{v'}\,dv'+\frac{\alpha_{AA}}{2}\int_0^v n(v')\times f(v-v')\,dv' \quad (14)$$

where $n(v)\,dv$ is the number of particles having volume between v and $v+dv$ and $f(v)$ is the corresponding particle fraction. Equation (14) can be expressed in discrete form. Numerical integration of the discrete form, using experimentally determined values of the respective probabilities, provides for comparison of predicted and observed particle size distributions[29] (Fig. 14). Agreement between predictions and observations is reason-

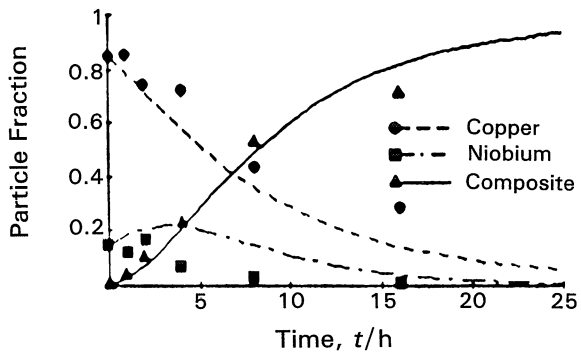

Fig. 13 Empirical fit, obtained through the kinetic model of Aikin, for attritor milling of an 85%Cu-15%Nb blend. Symbols represent experiment; the solid curves are "predictions". From (28).

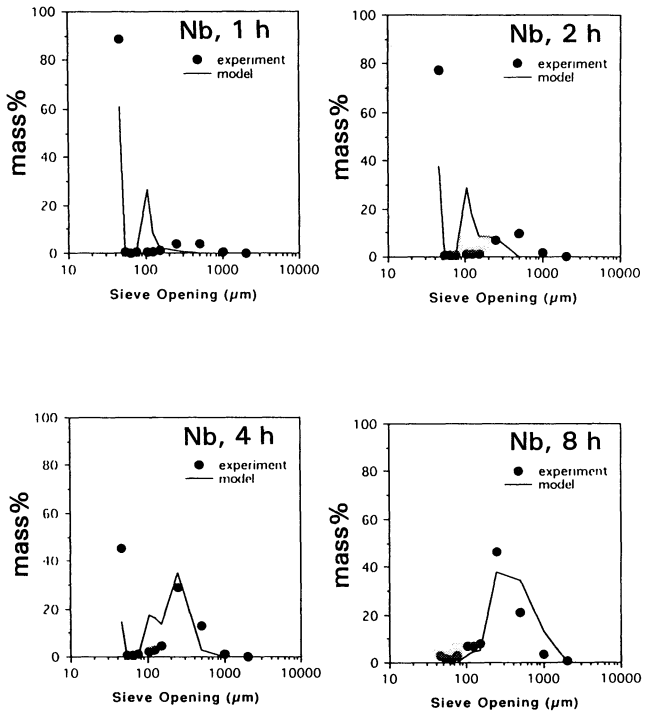

Fig. 14 Comparison of experimental and predicted particle size distributions for attritor milled Nb during the welding dominance stage of MA. Agreement between model and experimental results is reasonable for the longer milling times. From (29).

able. We caution that the analysis is restricted to the initial alloying stages, where the difference between the welding and fracture probabilities is approximately constant (cf. Fig. 4).

V. Global Modeling

Global modeling is useful in at least two respects. One, mentioned previously, is that knowledge of device specific media dynamics provides input for local modeling. This improves process modeling and may lead to process optimization. Another useful aspect of global modeling is that understanding of device specific media motion might result in improvements in device efficiency. Global modeling is discussed here from these perspectives. Results obtained in our laboratory, dealing with an attritor and a SPEX mill, are emphasized. However, as mentioned in the Introduction, there have been other noteworthy global modeling studies.

Rydin *et al*, using high speed cinematography, conducted a thorough study of the global dynamics of a transparent attritor[30]. Two primary types of media interaction are observed. One, termed direct impacts, is "high velocity" collisions between grinding balls. These impacts are prevalent in the attritor core, where the impeller arms are located. However, little of the powder charge is located in the core. Another type of impact, termed ball sliding[†15], is found in regions outside the core. Sliding results from differential rotational velocities between adjacent rows or columns of the grinding balls. The predominance of this type of action is a result of the close-packed array assumed by the grinding balls in the region outside of the attritor core. Frame- by-frame analysis of video recordings permitted the differences in velocities between adjacent rows (along the attritor walls) and columns (along the attritor bottom) to be quantitatively determined.

Powder was added to the transparent canister. Powder segregates substantially to the edge of the attritor bottom. This region of the attritor is termed the "dead zone" by Rydin *et al.*, as a result of the lack of ball motion there. The observations on powder distribution, when coupled with the media dynamic studies, show that an attritor is a very inefficient device. Not only are direct impacts restricted to its core (where little powder is present), but the region containing proportionally the most powder is characterized by a low frequency of ball-sliding.

From the standpoint of local modeling, the results of this study are of limited use. Most of the "collisions" take place in the attritor regions where the powder is most prevalent. However, these collisions are very ineffective for MA. Thus the effective collision velocity and frequency for use in local studies should not be those characteristic of the "dead zone." On the other hand, the velocity and frequency appropriate to local modeling are also not those of the attritor core, since so little powder is present there. Thus from the viewpoint of "improving" local modeling, the Rydin *et al.* study is useful only for reasonably "bracketing" an appropriate average velocity and frequency.

Rydin *et al.* suggested several ways for improving attritor efficiency. Among them was use of a mixture of differently sized balls in the mill. The idea is that this would result in a disruption of the close-packed array, thereby facilitating a greater incidence of direct impacts. Cook has conducted a study of attritor behavior when differently sized balls are used in the device[31]. When differently sized balls are placed in the attritor, the smaller balls segregate to the tank bottom at low device rotational velocities. Increasing this velocity reduces ball segregation and, at a critical rotational velocity (which is ball size, ball size ratio and tank diameter dependent), complete ball mixing takes place. Viewing video recordings of a transparent attritor shows that the close-packed array becomes "defective" when balls of different size are used. The defects are mainly "substitutional" or "interstitial" (depending on the radius ratio of the balls), although dislocations are sometimes observed.

Cook also measured alloying kinetics for attrition milling of Cu-Nb blends using differently sized balls and compared these to kinetics observed when milling was conducted with a single size grinding ball. Kinetics were estimated by measuring the time variation of the number of powder particles[†16]. Some of Cook's results are shown in Fig. 15. The logarithmic coordinates used in the figure do not adequately reflect the significant improvement in

[†15] Slow motion viewing of the videos shows that "ball sliding" is actually a manifestation of low velocity collisions.

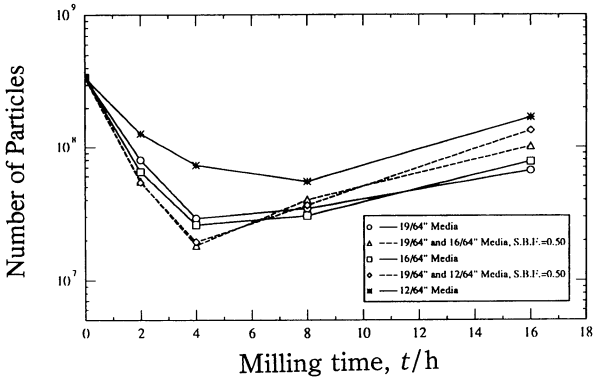

Fig. 15 Powder particle numbers as a function of processing time for a Cu-15 vol.%Nb powder blend during attritor milling. Relative to the situation when the same sized balls are used for milling, use of differently sized balls increases the net particle welding rate during the initial milling stages (through 4 h) and likewise increases the net particle fracture rate during the fracture domination stage (milling times in excess of 4 h) From (31).

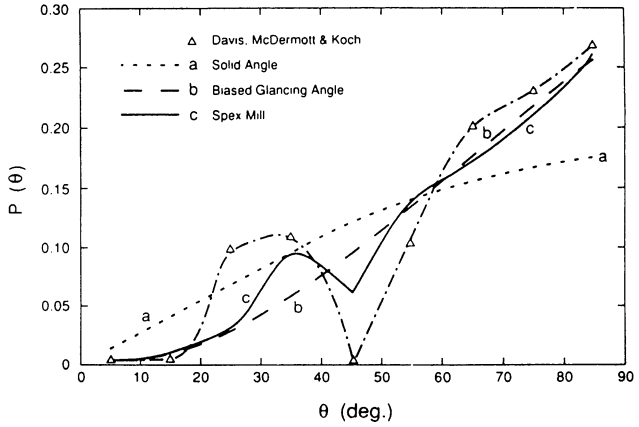

Fig. 16 Distribution in frequency of impact angles in a SPEX mill. $P(\theta)\Delta\theta$ represents the fraction of impacts taking place at an angle between θ and $\theta+\Delta\theta$ ($\theta=0$ corresponds to a "head-on" collision). Davis *et al.*'s experimentally determine distribution[32] is shown as are several calculated ones[16]. (Details relative to calculated distributions are provided in the text.) A combination of distribution (b) (biased glancing angle) and (c) (one ball model with ball-vial side/end collisions) qualitatively mimics the observed distribution. Note that very few collisions are "head-on" or nearly "head-on".

alloying kinetics obtained by using differently sized balls. The net welding rate (i.e., the difference between the welding and fracture rates) is increased by a factor of about two in the first 4 h of milling, as indicated by a factor of two decrease in particle numbers when milling with differently sized balls. Likewise, the net fracture rate for milling times greater than 4 h is about doubled when differently sized balls are used (as shown by a doubling in the rate of increase in particle numbers for milling times greater than 4 h). That the minimum in particle numbers occurs at approximately the same milling time, regardless of whether same or differently sized balls are used, suggests that the differently sized balls double both the welding and fracture rates (cf. Fig. 4). The improvement is also noteworthy in that it is by no means clear that either the optimum radius ratio of the differently sized balls or the optimum number fraction of the smaller sized balls were employed by Cook.

Media action within a transparent SPEX mill was photographically recorded by Davis *et al.*[32]. Relative collision frequencies as a function of impact angle are shown in Fig. 16. Only a small fraction of collisions is close to "head-on." Shown also in Fig. 16 are calculations of Courtney and Maurice for collision frequencies expected on several different geometrical bases. One basis assumes that the impact angle distribution is controlled by solid geometry consideration. This does not describe well the observed distribution. A distribution based on biased glancing angles mimics the actual distribution better. A third curve shown in Fig. 16 is based on a one ball mill; only collisions between the ball and the vial walls and ends are considered. This treatment predicts a relative minimum in impact frequency at an angle close to that found experimentally. Regardless of which distribution-or combination of distributions-best describes the observed one, it is clear that only a small fraction of media collisions in a SPEX mill are those for which MA takes place most rapidly.

If head-on collisions are most effective for MA, their frequency is the one that should be used in local modeling. How do we know (or why do we believe) head-on collisions are preeminent in effecting MA? For an attritor, this view is supported by observations (*e.g.*, Rydin *et al.*); for a SPEX mill, the conclusion is arrived at by deduction.

Davis *et al.* measured the coefficient of restitution (e) of balls in a SPEX mill; they found $e=0.72$. In the calculations summarized here, we have taken $e=0.7$. For this value of e, the maximum energy dissipated (through a head-on collision) is 0.225 times the precollision kinetic energy. Figure 17 illustrates the distribution in kinetic energy loss (in terms of the maximum possible energy loss) for the impact angle distributions of Fig. 16. Irrespective of the angular distribution, about 50% of media collisions result in an energy dissipation of less than 10% of the maximum one (i.e., about 2% of the precollision kinetic energy), and very few collisions result in an energy loss anywhere near the maximum possible one. Thus we deduce that only near head-on collisions result in significant energy dissipation in a SPEX mill, and these collisions are a small fraction of the total number of collisions. Here we have considered only kinetic energy losses in a mill without powder. Thus the approach is not directly translatable to the situation where energy is spent in deforming, welding and fracturing powder. However, it seems reasonable that the energy dissipated in action on the powder should scale with elastic

[†16] The absolute values of particle numbers are approximate, although the relative values can be used with confidence. Particle numbers are obtained by a sieve analysis, a technique necessary because of the large spread in processed particle sizes. Powder weights retained on different screens are converted to particle numbers by assuming spherically shaped particles.

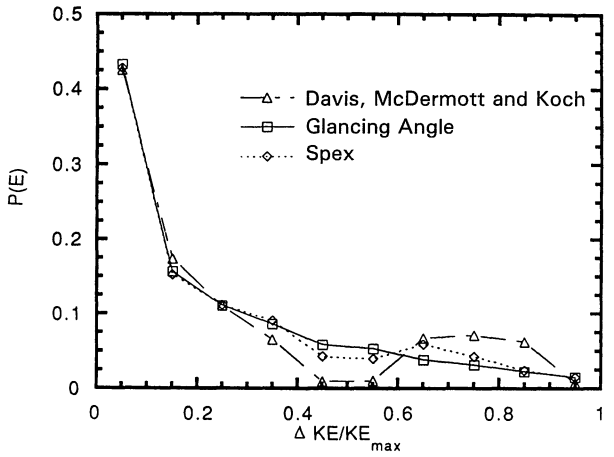

Fig. 17 Distribution in kinetic energy loss (for the impact angle distributions of Fig. 16) for inelastic collisions between balls having a coefficient of restitution, $e=0.7$ (for this value of e the maximum kinetic energy loss (KE_{max}) is 0.225 the precollision kinetic energy). Only a small fraction of collisions result in appreciable kinetic energy loss. In contrast nearly half of the collisions result in an energy loss about 1% of the precollision kinetic energy.

energy losses of the kind just considered. Thus we conclude that the collision velocity used in computational programs for local modeling of a SPEX mill should be the maximum velocity (corresponding to a head-on collision). This also justifies Maurice's use of a collision frequency in his programs that is much less than that pertaining to all media collisions. Finally, we note that these studies indicate that a SPEX mill is also inefficient. We sometimes think otherwise, but this is probably because of the high media velocity which characterizes a SPEX mill.

VI. Summary

A summary of recent efforts at modeling the mechanical and dynamical aspects of MA has been provided. The local modeling studies are useful for delineating important process parameters and, with appropriate empirical adjustment, can likely be used for "predictive" purposes. Global modeling has been fruitful in terms of noting inefficiencies in specific devices and thus has potential for improving the device efficiency. While there is significant room for further development of the models described, it is perhaps pertinent here to note that the local models can also be expanded to consider chemical effects happening during alloying[12]. To do this, though, requires establishment of a good data base of appropriate thermodynamic and kinetic parameters. At present, these are even more scarce than the corresponding mechanical data base apropos to MA conditions.

Acknowledgements

The Army Research Office (Dr. Edward Chen, grant monitor) has supported my efforts in this area. It is clear that several former graduate students-most notably David Maurice, Beverly Aikin and Richard Rydin-have contributed significantly to the modeling studies described here. However, other students and colleagues have engaged in related MA work which provides a necessary empirical basis for modeling of the process. In this regard, I particularly wish to thank Tomaz Kosmac, Alex Aning, Robert Comstock, Zhongang Wang, Robert Vance, Charles Mukira, Brian Murphy, Timothy Cook and Larry Henley.

REFERENCES

(1) A. K. Bhattacharya and E. Arzt: Scripta Metall. et Mater., **27** (1992), 749.
(2) R. M. Davis and C. C. Koch: Scripta Metall. et Mater., **21** (1987), 305.
(3) R. B. Schwarz and C. C. Koch: Appl. Phys. Letters, **49** (1986), 146.
(4) N. Burgio, A. Iasonna, M. Magini, S. Martelli and F. Padella: II Nuovo Cimento, **13D** (1991), 459.
(5) P. G. McCormick, H. Huang, M. P. Dallimore, J. Ding and J. Pan: *Proc. 2nd Intl. Conf. on Structural Applications of Mechanical Alloying*, Ed. by J. J. DeBarbadillo, F. H. Froes and R. Schwarz, ASM Intl., Materials Park, O., (1993), p. 45.
(6) A. K. Bhattacharya and E. Arzt: Scripta Metall. et Mater., **28** (1993), 395.
(7) M. Atzmon: Metall. Trans. A., **23A** (1992), 49.
(8) G. B. Schaeffer and P. G. McCormick: Metall. Trans. A, **23A** (1992), 1285.
(9) G. B. Schaeffer and P. G. McCormick: Metall. Trans. A, **22A** (1991), 3019.
(10) E. Gaffet: Mater. Sc. and Eng., **A119** (1989), 185.
(11) A. K. Bhattacharya and E. Arzt: Scripta Metall. et Mater., **27** (1992), 635.
(12) T. Kosmac, D. Maurice and T. H. Courtney: J. Am. Cer. Soc., **76** (1992), 2345.
(13) E. Artz, M. F. Ashby and K. E. Easterling: Metall. Trans. A, **14A** (1983), 211.
(14) A. S. Helle, K. E. Easterling and M. F. Ashby: Acta Metall., **26** (1985), 2163.
(15) D. R. Maurice and T. H. Courtney: Metall. Trans. A, **21A** (1990), 289.
(16) T. H. Courtney and D. R. Maurice: *Solid State Powder Processing*, Ed. by A. H. Clauer and J. J. deBarbadillo, TMS, Warrendale, Pa., (1989), p. 3.
(17) D. Maurice: Ph. D. Thesis, University of Virginia, (1992).
(18) D. Maurice and T. H. Courtney: Metall. and Mater. Trans. A, **25A** (1994), 147.
(19) D. Maurice and T. H. Courtney: submitted for publication.
(20) N. Bay: Weld. J., **62** (1983), 137s.
(21) N. Bay: J. Eng. Ind., **101** (1979), 121.
(22) H. A. Mohamed and J. Washburn: Weld. J., **54** (1975), 302s.
(23) B. J. M. Aikin: Ph. D. Thesis, University of Virginia, (1992).
(24) B. Avitzur: *Metal Forming: Processes and Analysis*, R. E. Krieger Co., Huntington, N. Y., (1979), p. 77.
(25) J. S. Benjamin and T. E. Volin: Metall. Trans., **5** (1974), 1929.
(26) P. S. Gilman and W. D. Nix: Metall. Trans. A, **12A** (1981), 813.
(27) B. J. M. Aikin, T. H. Courtney and D. R. Maurice: Mater. Sc. and Eng., **A147** (1991), 229.
(28) B. J. M. Aikin and T. H. Courtney: Metall. Trans. A, **24A** (1993), 647.
(29) B. J. M. Aikin and T. H. Courtney: Metall. Trans. A, **24A** (1993), 2465.
(30) R. M. Rydin, D. Maurice and T. H. Courtney: Metall. Trans. A, **24A** (1993), 175.
(31) T. M. Cook: M. S. Thesis, Michigan Technological University, (1994).
(32) R. M. Davis, B. McDermott and C. C. Koch: Metall. Trans. A, **19A** (1988), 2867.